LA-UR/98- -3567

Approved for public release; distribution is unlimited.

TITLE: STRESS-INDUCED MARTENSITIC TRANSFORMATIONS IN NITI AND NITI-TIC COMPOSITES INVESTIGATED BY NEUTRON DIFFRACTION

AUTHOR(S): R. Vaidyanathan, MIT
M.A.M. Bourke, MST-8
D.C. Dunand, Northwestern University

SUBMITTED TO: ICOMAT '98 published in Material Science & Engineering A

Los Alamos
NATIONAL LABORATORY

DISCLAIMER

accepted for presentation at ICOMAT '98
proceedings to be published in Mat Sci & Eng A

Stress-Induced Martensitic Transformations in NiTi and NiTi-TiC Composites Investigated by Neutron Diffraction

R. Vaidyanathan
Department of Materials Science and Engineering
Massachusetts Institute of Technology, USA

M.A.M. Bourke
LANSCE/MST
Los Alamos National Laboratory, USA

D.C. Dunand
Department of Materials Science and Engineering
Northwestern University, USA

Superelastic NiTi (51.0 at% Ni) with 0, 10 and 20 vol% TiC particles were deformed under uniaxial compression as neutron diffraction spectra were simultaneously obtained. The experiments yielded in-situ measurements of the thermoelastic stress-induced transformation. A detailed Rietveld [1] determination is made of the phase fractions and the evolving strains in the reinforcing TiC particles and the austenite as it transforms to martensite on loading (and its subsequent back transformation on unloading). These strains are used to shed light on the phenomenon of load transfer in composites where the matrix undergoes a stress-induced phase transformation.

1 Introduction

Unlike metal matrix composites where the matrix primarily deforms by slip, composites where the matrix deforms by alternative mechanisms (e.g. twinning or stress-induced transformations) have been little studied. The intermetallic NiTi with near-equiatomic composition deforms by such mechanisms because of its reversible, thermoelastic transformation between a high-temperature, cubic (B2) parent austenitic phase and a low-temperature, monoclinic (B19) martensitic

phase [2]. Dunand and co-workers have carried out a series of investigations to systematically characterize such NiTi based shape-memory composites where a martensitic NiTi matrix deforms by twinning in the presence of TiC particles [3-7]. However, to the best of our knowledge, no study exists on the mechanical behavior of NiTi-based composites where an austenitic matrix deforms by stress-induced martensite in the presence of a reinforcing ceramic phase. We recently demonstrated the ability to observe stress-induced transformations in NiTi by subjecting mechanically-loaded NiTi samples to neutron diffraction [8]. In the present paper, we use this technique to investigate the evolution of martensite fractions and discrete phase strains in superelastic austenitic NiTi and NiTi-TiC composites under compression loading.

2 Experimental procedures

Details of sample characterization and fabrication by hot-isostatic-pressing (HIP) of prealloyed NiTi (51.0 at% Ni) powders are described elsewhere [9]. Three types of materials were used with the following compositions: (a) unreinforced NiTi (b) NiTi with 10 volume % TiC; and (c) NiTi with 20 volume % TiC, hereafter referred to as NiTi, NiTi-10TiC and NiTi-20TiC. Cylindrical samples (10 mm in diameter and 24 mm in length) were solutionized in titanium-gettered flowing argon at 1000∞C for one hour, oil-quenched to room temperature, annealed at 400∞C for one hour in air and quenched in ice-water. An average grain-size of 20 μm was measured for all three materials which exhibited a stable austenitic phase at room temperature.

Detailed information on the experimental setup can be found elsewhere [6, 10] and is only summarized here. Neutron diffraction measurements were performed in "time of flight" mode using the Neutron Powder Diffractometer (NPD) at the pulsed neutron source at Los Alamos National Laboratory. The samples were subjected to uniaxial compressive stresses at room temperature while

neutron diffraction spectra were acquired in three scattering geometries. The loading axis formed an angle of 45∞ with the incident neutron beam, allowingmeasurements for which the scattering vectors were parallel and perpendicular to the loading axis. Since the incident beam is monochromatic, by choosing data from the appropriate bank of detectors, information from planes parallel or perpendicular to the loading direction can be obtained. In addition, a third detector was used in back-scattering geometry and provided a measurement between the other two. An extensometer was attached to the cylindrical compression samples so that macroscopic strain was recorded during the experiments.

Fig. 1 shows the stress-strain curves of the samples indicating the stress levels at which neutron spectra were obtained. After the load was stabilized, the samples accumulated strain before reaching (within a few minutes) the strain levels marked with black dots. This effect can be attributed to the relatively high loading rate which did not allow sufficient time for transformation enthalpy dissipation [11-13]. Since the transformation is thermoelastic, on equilibrating to a lower uniform temperature, a strain is produced. This phenomenon had no significant effect on the neutron measurements due to the long acquisition time of about 6 hours. The load-unload cycles in Fig. 1 were obtained after training the sample twice to 625 MPa at a stroke speed of 3 mm/min in order to stabilize the transformation by removing any instabilities or heterogeneities that may exist.

3 Neutron diffraction data analysis

By using a Rietveld refinement [1] technique in the Los Alamos National Laboratory code GSAS [14], analysis is not limited to individual lattice plane reflections which may not be representative of the overall deformation of the polycrystal. In the Rietveld refinement method, a mathematical model is developed that calculates an intensity, Y_c, at every point in the spectra, i.e.

$$Y_c = Y_b + \sum_h SKF_h^2 P(\Delta T_h) \quad \text{..... 1}$$

where the first term, Y_b, is the background intensity and the second term is the Bragg scattering containing a structure factor, F_h, a scale factor, S, a correction factor, K, and a profile function, $P(\Delta T_h)$, as determined by the displacement, ΔT_h, of the profile point from the reflection position. Within the correction factor K is a term which describes the change in Bragg intensity for a reflection due to texture. The refinement procedure varies various parameters related to phase volume fractions, atom positions and texture, until the calculated spectrum matches the measured spectrum in a least squares fit.

The strains are described by an average isotropic strain along <100>, i.e. a parameter α that shifts individual lattice reflections (peaks) according to a changes in the lattice constant so that

$$\varepsilon \approx \varepsilon_{h00} \equiv \frac{\alpha}{C} \quad \text{..... 2}$$

where C is the diffraction constant for the instrument (since the peak position change is in units of time in the case of time of flight data). A more rigorous analysis of neutron spectra obtained from NiTi is carried out and described in detail in Ref. [15] and shows the above strain description to give an average isotropic representation of the individual lattice plane behavior. The texture of the stress-induced martensite is formulated using a generalized spherical harmonics description [16, 17].

4 Results and Discussion

An unreacted NiTi-TiC interface was observed by optical microscopy, confirming the inertness of the TiC particles, which show an almost perfectly stoichiometric composition of 49.8 ± 0.1 at% C, as determined by combustion analysis with infrared detection. Refs. [18, 19] also report no reaction over a large range of compositions in the NiTi-TiC system and Ref. [3] use microprobe

analysis to draw the same conclusions in martensitic NiTi-TiC composites. Given the inert nature of the TiC and the identical initial materials and processing routes for all samples, the NiTi matrix chemical composition can be assumed constant in all samples, suggesting that the differences in mechanical behavior observed in Fig. 1 are not due to chemical effects.

Fig. 2 compares normalized neutron spectra for lattice planes perpendicular to the loading direction. Qualitative comparison of the martensite peaks at 625 MPa shows that the amount of martensite decreases with increasing TiC content. Using a generalized spherical harmonics texture formulation in a Rietveld refinement of diffraction data from all three sets of detectors, the volume fraction of martensite in NiTi and NiTi-10TiC was quantified as a function of the applied external stress, as shown in Fig. 3. For NiTi-20TiC, the volume fraction of martensite present was too small (< 5 vol% at max. load) for the refinement to converge. The difference in macroscopic strain-stress curves observed in NiTi and NiTi-10TiC and NiTi-20TiC (Fig. 1) may thus be attributed to the differences in martensite volume fractions formed under stress.

Table 1 shows the elastic modulus for the three specimens as determined from extensometer data. The values are obtained from a linear fit to the region prior to the onset of non-linearity in the curves in Fig. 1. Table 1 also shows predictions using values reported from the literature. Using stiffness tensor values from ultrasonic measurements of single crystals from Ref. [20], the Young's modulus of the polycrystal is determined as a single-crystal average using Hashin-Shtrikman [21] upper and lower bounds for cubic polycrystals. The bounds for NiTi are very tight and predict moduli of 74.4 and 75.4 GPa. The Voigt and Reuss average suggested by Hill [22] gives a modulus of 74.5 GPa. Using slightly different single-crystal data from Ref. [23], the Hashin-Shtrikman upper and lower bounds and the Hill average are 72.9 GPa, 74.3 GPa and 73.0 GPa, respectively. The values predicted for the composite are obtained from the Eshelby equivalent inclusion method

outlined in Refs. [24] and [6] with elastic TiC data from Ref. [25]. In predicting an average modulus for the composite, coefficient of thermal expansion (CTE) mismatch stresses between austenitic NiTi and TiC are neglected because of their low values: the average matrix tensile stress is 24.9 MPa in NiTi-10TiC and 49.1 MPa in NiTi-20TiC from the above method, assuming a temperature drop of 731 K and CTE values from Refs. [26, 27]. Table 1 shows a significant difference between the predicted moduli and those obtained from extensometer measurements. This discrepancy cannot be explained by texture in the austenite since Rietveld refinements indicate no texture at these low load levels. The predictions account for purely elastic contributions to the modulus while the extensometer may measure non-elastic contributions, i.e. strains due to the stress-induced transformation. Thus the difference in Table 1 can be attributed to austenite transforming to martensite at low stresses in amounts proportional to the applied stress, thus reducing the apparent Young's modulus. Since the strains generated by the austenite-martensite transformation are large even a small volume fraction of martensite can account for the observed differences. Assuming that favorable orientations of austenite transform to martensite at these low stresses (producing e.g. a compressive strain of 5.2% in the <011> direction with reference to the parent phase vector basis [28]), a mere 1 vol % of martensite is needed every 71.6 MPa to explain the difference in Young's moduli for NiTi in Table 1. This small volume fraction can be detected neither by refinement methods nor by qualitative examination of single peaks in spectra because the low-symmetry martensite shows a large number peaks with low intensities.

Fig. 4 shows the longitudinal strain from planes perpendicular to the loading direction obtained from the Rietveld analysis (Eq. 2) in the unreinforced NiTi during loading and unloading. The average modulus is 74.5 GPa, in very good agreement with the values obtained from the various averaging methods (Table 1). The modulus of the austenite phase measured by this method can be

expected to change at higher load levels due to: (i) load transfer to the stress-induced martensite which exhibits different elastic constants, (ii) transformation mismatch stresses between the two phases, and (iii) the evolving texture in the austenite. The latter effect results from the strong texture qualitatively observed in individual spectra of the stress-induced martensite. Since a unique lattice correspondence exists between the austenite and the martensite phases, the austenite is expected to develop texture as well. However, Fig. 4 shows that these three effects do not cause any significant non-linearity in the stress-strain response of austenite in neither loading or unloading, despite the fact that more martensite exists during unloading than loading for the same stress level due to the hysteresis shown in Fig. 1 and Fig. 3. This suggests that the non-linear effects either cancel each other or have negligible magnitude.

Fig. 5 and Fig. 6 show individual phase strains in the austenite matrix and TiC reinforcement in the composites as obtained by the Rietveld refinement (using Eq. 2 for data from lattice planes perpendicular to the loading direction) and as predicted from the Eshelby elastic theory. The Eshelby prediction takes into account the mismatch in the coefficient of thermal expansion between austenitic NiTi and TiC for the initial residual stain (no applied stress) and the mismatch in elastic stiffness for the phase strains under applied external stress. Values obtained from the single-crystal averaging methods for austenitic NiTi were used to represent the matrix in the predictions, in the light of its behavior in Fig. 4 and values from Ref. [25] for TiC. Fig. 5 and Fig. 6 show reasonable agreement between the elastic theory and the measurements. Agreement in Fig. 6 is expected for NiTi-20TiC because little martensite is formed and the composite deforms mostly elastically. On the other hand, NiTi-10TiC shows significant amounts of stress-induced martensite at high applied stresses (Fig. 3) which could lead to additional mismatch with the TiC particulate and deviation from the elastic response in Fig. 5, as observed in plastically deforming aluminum composites [29]. The lack of such

plastic load-transfer suggests that the austenite/martensite matrix effectively accommodates the mismatch arising due to the large transformation strains associated with the transformation. This may be attributed to the self-accommodating nature of the transformation wherein certain variants can preferentially transform, as also observed in shape-memory NiTi composites deforming by martensite twinning. [4]

A companion publication [9] investigating in detail the texture, phase fraction and strain evolution in these materials at higher applied stresses will be published separately.

5 Conclusions

It has been demonstrated that Rietveld refinements from neutron diffraction spectra can be used to investigate stress-induced transformations in superelastic NiTi. The generalized spherical harmonics texture formulation allows for accurate determination of the evolving phase fractions. The volume of martensite formed decreases with increasing TiC content. The simple strain formulation sheds lights on the load transfer mechanisms. Excellent agreement is observed between Eshelby elastic theory in the austenitic NiTi matrix and TiC suggesting that the self-accommodation of the martensite results in the mismatch due to the transformation strains not being very significant.

Acknowledgements

The Manuel Lujan Jr. Neutron Scattering Center is a national user facility funded by the US DOE (Contract No. W-7405-ENG-36) and by Defense Programs. RV and DCD acknowledge the support of Daimler Benz AG in the form of a research grant. The authors also thank Drs. H. Pettermann and M.R. Daymond for helpful discussions.

List of Figures

	Extensometer measurement	Theoretical prediction	Method of prediction
NiTi	50 ± 2	74.4-75.4 74.5	Hashin-Shtrikman [21] Hill average [22]
NiTi-10TiC	58 ± 2	90.9	Eshelby[24]
NiTi-20TiC	74 ± 2	96.5	Eshelby[24]

Table 1: Young's moduli (GPa) of NiTi, NiTi-10TiC and NiTi-20TiC as determined from extensometry and as predicted from literature values; discrepancies suggest non-elastic contributions to the extensometer moduli.

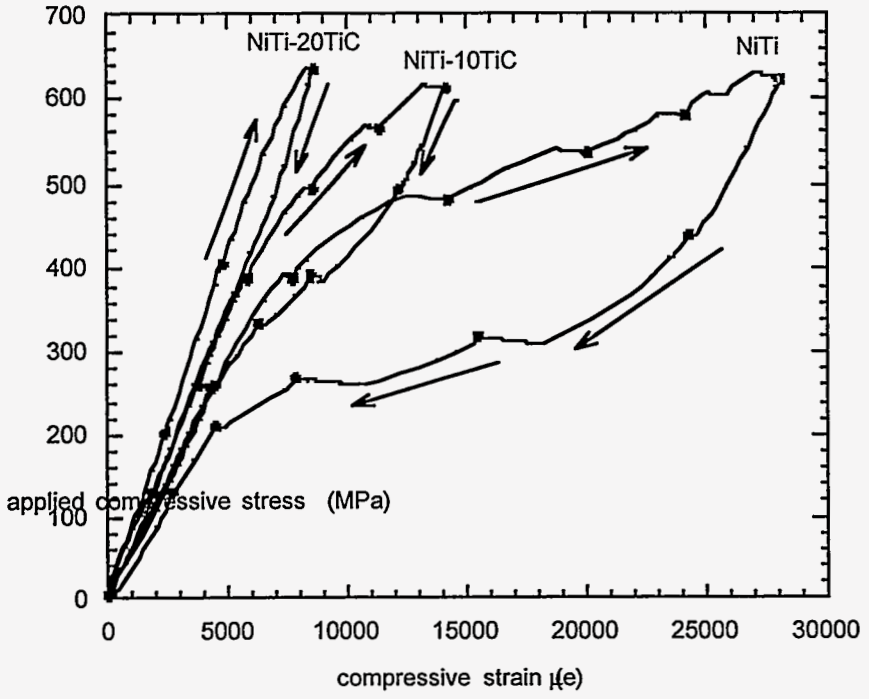

Fig. 1 Compressive stress-strain curves of NiTi, NiTi-10TiC and NiTi-20TiC. The plateaus indicate the stress levels at which neutron diffraction spectra were obtained; the samples settled rapidly to the strain levels marked with dots.

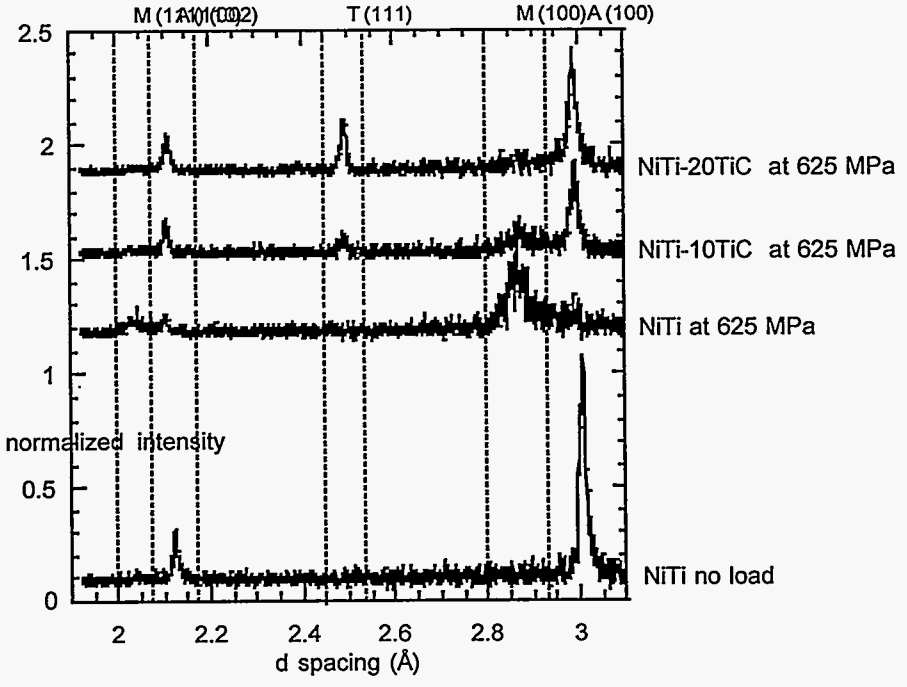

Fig. 2 Section of normalized neutron diffraction spectra from NiTi, NiTi-10TiC and NiTi-20TiC at 625 MPa compared to the spectra of NiTi at no load with the austenite (A), martensite (M) and TiC (T) peaks identified.

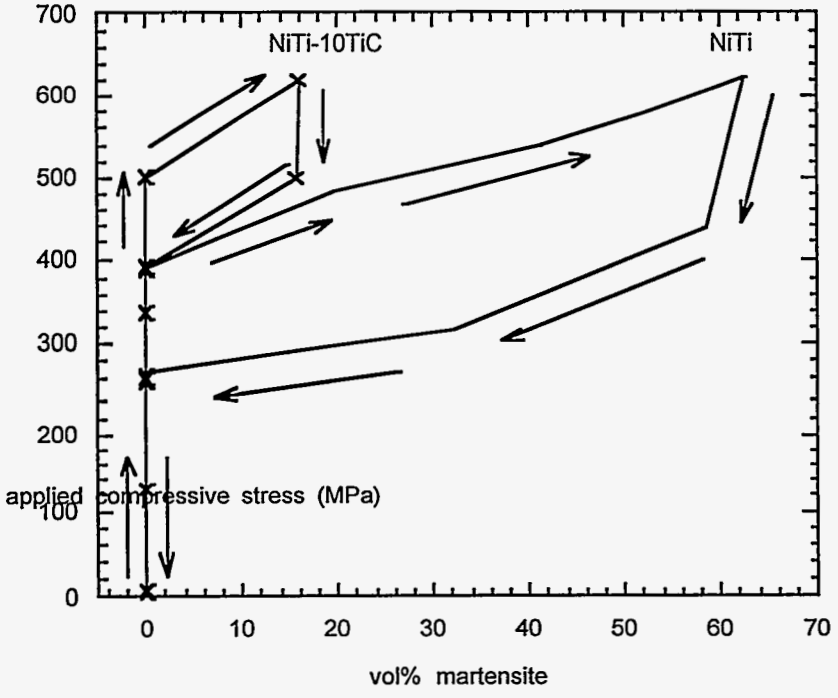

Fig. 3 Volume fraction of martensite obtained from Rietveld refinements as a function of the applied stress in NiTi and NiTi-10TiC.

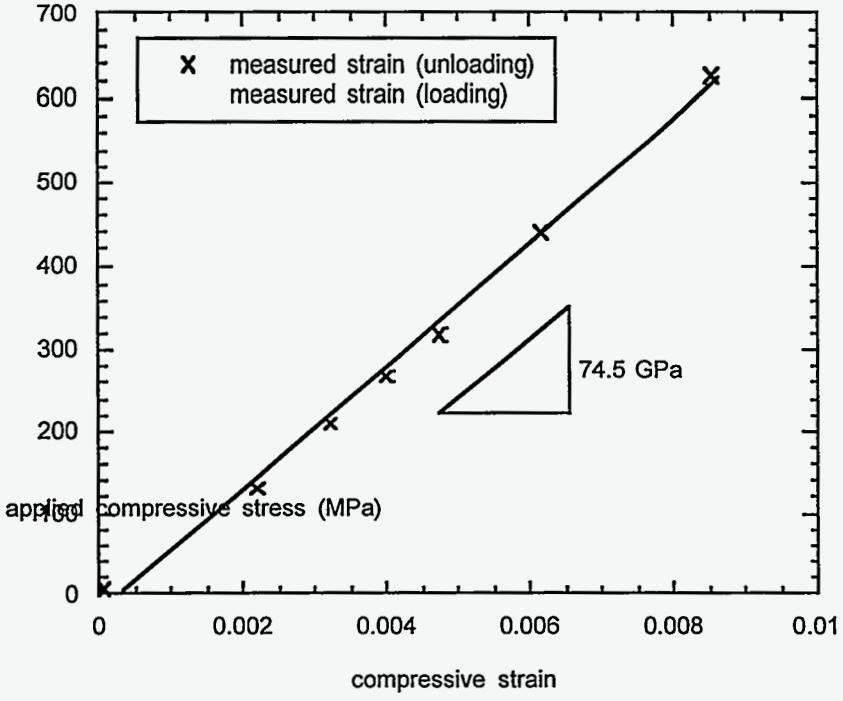

Fig. 4 Plot of applied stress versus axial strain in the austenitic phase of NiTi, as obtained from Rietveld refinements.

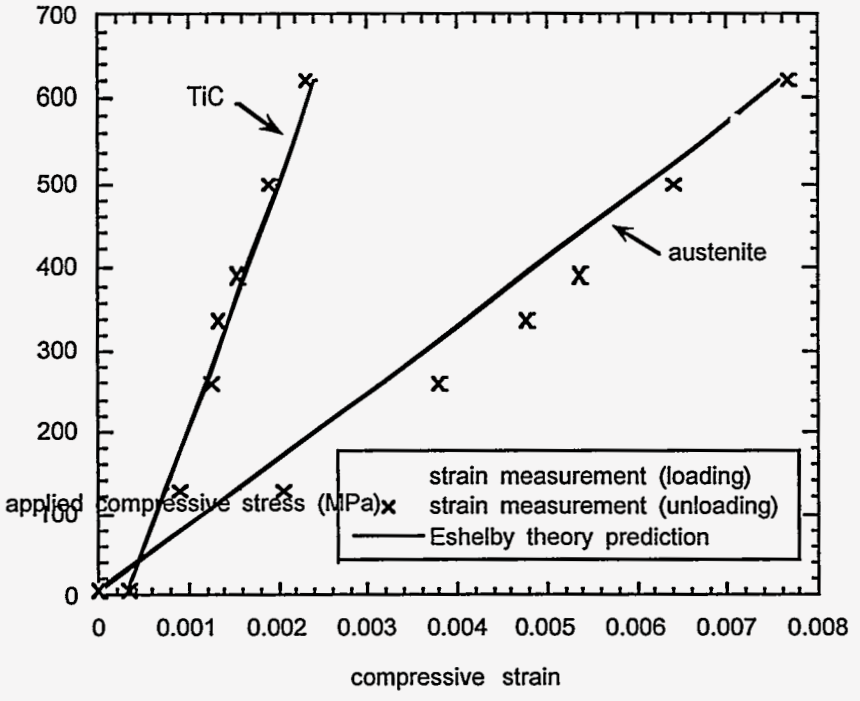

Fig. 5 Measured and predicted (Eshelby theory) axial strains in the matrix austenitic phase and in the TiC reinforcement for NiTi-10TiC.

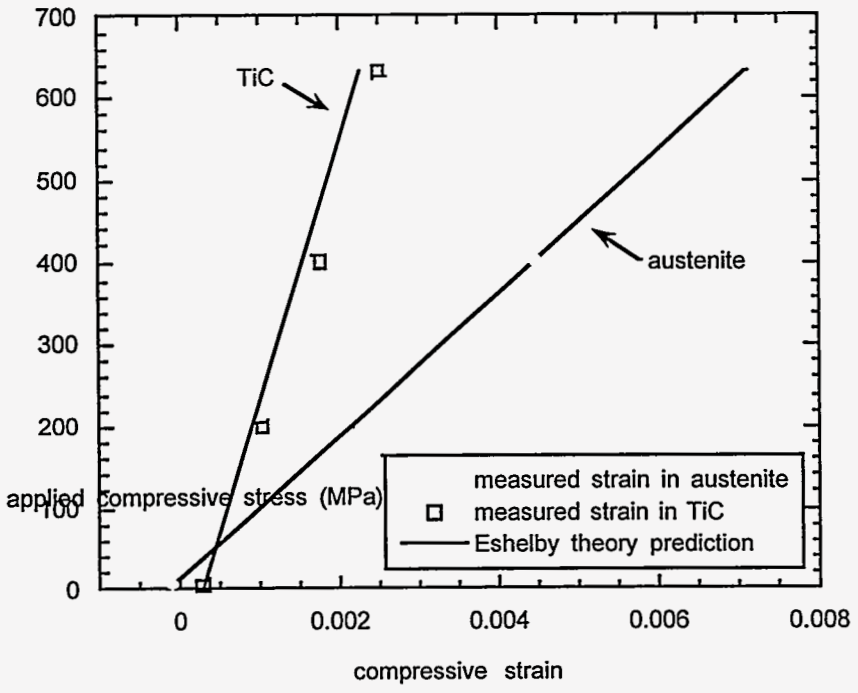

Fig. 6 Measured and predicted (Eshelby theory) axial strains in the matrix austenitic phase and in the TiC reinforcement for NiTi-20TiC..

References

[1] H. M. Rietveld, *J. Appl. Crystallogr.*, vol. 2, pp. 65, 1969.

[2] T. W. Duerig, K. N. Melton, D. Stoeckel, and C. M. Wayman, "Engineering Aspects of Shape Memory Alloys," . London: Butterworth-Heinemann, 1990.

[3] D. Mari and D. C. Dunand, *Metall. Mater. Trans.*, vol. 26A, pp. 2833, 1995.

[4] K. L. Fukami-Ushiro and D. C. Dunand, *Metall. Mater. Trans.*, vol. 27A, pp. 183, 1996.

[5] K. L. Fukami-Ushiro, D. Mari, and D. C. Dunand, *Metall. Mater. Trans.*, vol. 27A, pp. 193, 1996.

[6] D. C. Dunand, D. Mari, M. A. M. Bourke, and J. A. Roberts, *Metall. Mater. Trans.*, vol. 27A, pp. 2820, 1996.

[7] D. C. Dunand, K. L. Fukami-Ushiro, D. Mari, J. A. Roberts, and M. A. M. Bourke, in *Advances in Materials for Smart Systems (MRS 1996 Fall meeting)*, 1996.

[8] M. A. M. Bourke, R. Vaidyanathan, and D. C. Dunand, *Appl. Phys. Lett.*, vol. 69, pp. 2477, 1996.

[9] R. Vaidyanathan, M. A. M. Bourke, and D. C. Dunand, *Study of superelastic NiTi and NiTi-TiC using neutron diffraction , to be submitted to Acta Mat.*, 1998.

[10] N. Shi, M. A. M. Bourke, J. A. Roberts, and J. E. Allison, *Metall. Mater. Trans.*, vol. 28A, pp. 2741, 1997.

[11] P. H. Leo, T. W. Shield, and O. P. Bruno, *Acta Metall. Mater.*, vol. 41, pp. 2477, 1993.

[12] S. Miyazaki, K. Otsuka, and Y. Suzuki, *Scripta Metall.*, vol. 15, pp. 287, 1981.

[13] P. G. McCormick and Y. Liu, *Mat. Sci. Eng.*, vol. A167, pp. 51, 1993.

[14] A. C. Larson and R. B. V. Dreele, "General Structure Analysis System (GSAS)," Los Alamos National Laboratory LAUR 8-748, 1986.

[15] R. Vaidyanathan, M. A. M. Bourke, and D. C. Dunand, *Analysis of neutron diffraction spectra obtained during stress-induced transformations in superelastic NiTi, to be submitted to Journal of Applied Physics*, 1998.

[16] H. J. Bunge, *Texture Analysis in Materials Science*. London: Butterworth, 1982.

[17] R. B. V. Dreele, *J. Appl. Cryst.*, vol. 30, pp. 517, 1997.

[18] T. M. Poletika, S. N. Kulkov, and V. E. Panin, *Poroshkova Metallurgiya*, vol. 7 (247), pp. 54, 1983.

[19] S. N. Kulkov, T. M. Poletika, A. Y. Chukhlomin, and V. E. Panin, *Poroshkovaya Metallurgiya*, vol. 8 (260), pp. 88, 1984.

[20] T. M. Brill, S. Mittelbach, W. Assmus, M. Muellner, and B. Luethi, *J. Phys.: Condens. Matter*, vol. 3, pp. 9621, 1991.

[21] Z. Hashin and S. Shtrikman, *J. Mech. Phys. Solids*, vol. 10, pp. 335, 1962.

[22] R. Hill, *Proc. Phys. Soc (London)*, vol. A65, pp. 349, 1952.

[23] O. Mercier, K. N. Melton, G. Gremaud, and J. Haegi, *J. Appl. Phys.*, vol. 51 (3), pp. 1833, 1980.

[24] T. W. Clyne and P. J. Withers, *An Introduction to Metal Matrix Composites*: Cambridge University Press, UK, 1993.

[25] R. Chang and L. J. Graham, *J. Appl. Phys.*, vol. 37, pp. 3778, 1966.

[26] C. M. Jackson, H. J. Wagner, and R. J. Wasilewski, "NASA-SP 5110," 1972.

[27] J. Shackelford and W. Alexander, "The CRC Materials Science and Engineering Book," . Boca Raton, FL: CRC Press, 1992, pp. 358.

[28] T. Saburi and S. Nenno, "Solid-Solid Phase Transformations," , 1981.

[29] M. A. M. Bourke, J. A. Goldstone, N. Shi, J. E. Allison, M. G. Stout, and A. C. Lawson, *Scripta Metall. Mater.*, vol. 29, pp. 771, 1993.